

# Impact Strength Measurement Rig For Construction Materials: Using Astm F3007-13 Standard

**Sangeetha N<sup>1\*</sup> Santhiya S<sup>2</sup>, Kalanithi S<sup>2</sup>**

*<sup>1,2</sup> Department Mechanical Engineering, Kumaraguru College of Technology, Tamil Nadu, India, 641049 \*E-mail address: [sangeetha.n.mec@kct.ac.in](mailto:sangeetha.n.mec@kct.ac.in)*

The development of an impact strength measurement rig is crucial for evaluating the mechanical properties of construction materials under sudden loading conditions. This study focuses on designing and fabricating a ball drop test rig based on the ASTM F3007-13 standard to experimentally measure and validate impact strength against finite element method (FEM) simulations in ANSYS. The rig features an electromagnetic fixture for securely holding various ball sizes and a lead screw mechanism for precise drop height adjustments, ensuring standardized testing. Additionally, a digital impact measurement system, integrating a microphone and a high-speed camera, enhances the accuracy of material behavior analysis. Experimental and simulation studies conducted on 20 mm thick architectural glass evaluated the rebound velocity of a steel ball after impact, with microphone-based measurements recording 2.65 m/s, high-speed camera measurements capturing 2.25 m/s, and FEM simulations predicting 2.75 m/s. The close correlation between these results confirms the accuracy and efficiency of the test rig in assessing the impact resistance of construction materials.

**Key words:** Ball drop test, Impact test rig design, Collision, Rebound velocity, Architectural glass.

## 1. INTRODUCTION

The impact strength of construction materials is crucial in determining their durability under sudden loading conditions. Various structural components, such as glass panels, metal sheets, and composites, must withstand impact forces in buildings, transportation, and industrial infrastructure. Evaluating impact strength requires standardized testing to ensure reliability and compliance with industry standards like ASTM F3007-13.

Architectural glass, widely used in modern construction, remains vulnerable to impact forces that may cause fragmentation. Ge, Li, and Chen examined glass panel fragmentation under blast loading, emphasizing the need for reliable impact testing [1]. Similarly, studies have shown that impact resistance varies based on material composition and structural properties [2]. Standardized tests like Charpy and Izod have been extensively used for cementitious composites and polymer materials to evaluate fracture resistance [3,4].

The development of specialized impact test rigs enhances measurement precision and experimental repeatability. Jurecki et al. highlighted the importance of controlled testing environments for mechanical property evaluation [5]. This study focuses on constructing a ball drop test rig based on ASTM F3007-13 to assess impact strength. This rig includes an electromagnetic fixture for securing various ball sizes and a lead screw mechanism for adjustable drop height. Additionally, digital measurement systems, such as microphones and high-speed cameras, ensure accurate impact analysis. Pisano, Bonati, and Royer-Carfagni investigated the effect of size and stress state on the strength of architectural glass, demonstrating how material behavior can be influenced by various factors [6]. Similar approaches have been utilized in experimental studies on tempered glass panels and LCD cover glass [7,8].

A critical aspect of this research is validating experimental results against numerical simulations using FEM in ANSYS. Previous studies have demonstrated the effectiveness of numerical modelling in predicting impact response, fracture behaviour, and energy dissipation [6,9]. Provides details on using video analysis for bounce measurement in table tennis, which aligns with this impact strength measurement system[10]. This study evaluates the rebound velocity of a steel ball impacting 20 mm thick architectural glass. As impact testing evolves, innovative test rigs will be essential in advancing material science and engineering applications.

## **2. IMPACT STRENGTH BY BALL DROP TEST**

The impact strength of a material in a ball drop test is influenced by conservation of energy, conservation of momentum, and material deformation characteristics. A mass is dropped from a predetermined height onto a material specimen, transferring energy through plastic and elastic deformation. The extent of energy absorption and restitution determines impact resistance [14].

Upon impact, part of the kinetic energy dissipates through plastic deformation, forming permanent dents, while the remaining energy is stored elastically, allowing the mass to rebound. The rebound height determines the coefficient of restitution, which quantifies energy recovery efficiency after impact. This coefficient, defined as the ratio of rebound velocity to initial velocity, is crucial for assessing material impact resistance [15,16]. The study on rockfall experiments and the coefficient of restitution, which aligns with on impact testing[11]. Traditional measuring instruments, such as high-speed cameras and slope cushions with additional sensors, often introduce errors in coefficient measurement [12]. Yang et al. developed an innovative test device that directly monitors trajectory parameters, including linear and angular acceleration, in real time with high accuracy. Their study highlights the influence of incidence velocity, slope lithology, and incidence angles on the coefficient of restitution, providing valuable insights for impact assessment and mitigation engineering [13]

Studies have examined impact dynamics and material response. Qiao et al. [14] reviewed high-energy absorbing materials, emphasizing controlled deformation for impact energy dissipation. Similarly, Zafar et al. [15] proposed measuring particle adhesion force based on energy loss in

drop tests, highlighting the importance of energy dissipation mechanisms in material characterization.

The coefficient of restitution evaluates energy retention and dissipation properties [17,18]. Lower values indicate higher energy absorption, typical of ductile materials, while higher values signify increased elasticity and minimal energy loss. Experimental studies on metals, glass, and polymers reveal distinct impact behaviours based on microstructural properties and failure modes [8,9]. Sandeep et al. [19] conducted an experimental study on the coefficient of restitution for various natural and engineered materials, further emphasizing the role of grain properties and interface conditions in impact resistance. Their findings contribute to a deeper understanding of material behaviour under repeated impact loading conditions.

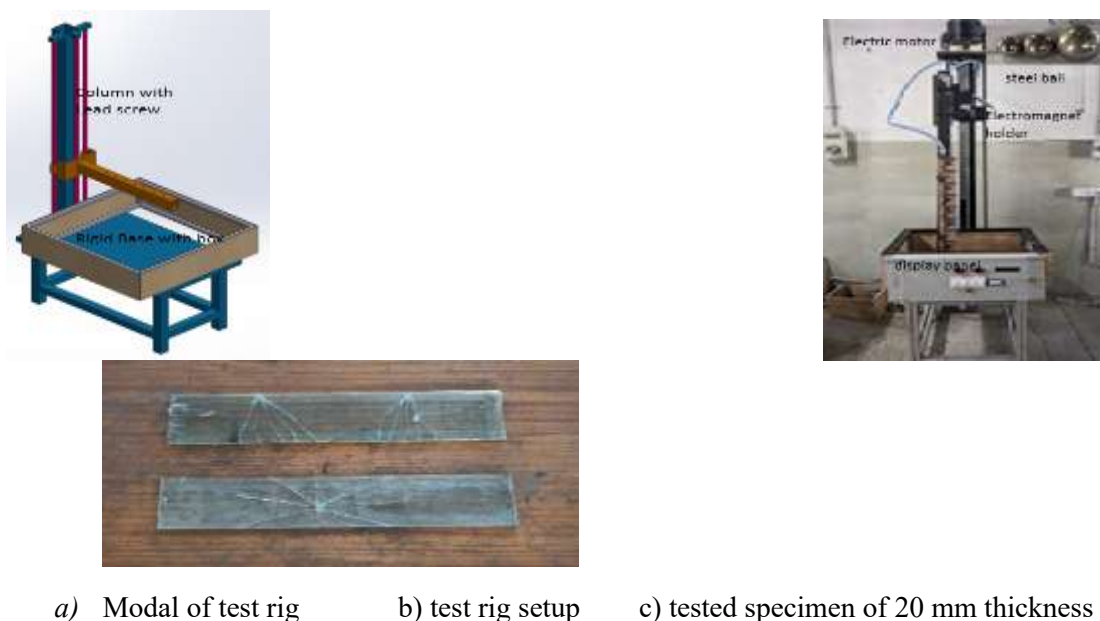
In summary, the ball drop test provides a reliable method for evaluating material impact strength by analysing energy transfer, deformation behaviour, and restitution characteristics. This assessment aids in material selection and design optimization for applications requiring durability and energy absorption capabilities.

### **3. DESIGN AND DEVELOPMENT OF AN IMPACT TEST RIG**

Ball impact testing has been a traditional method for assessing glass safety. The test rig has been designed in accordance with the ASTM 3007 standard. Prior to fabrication, a model of the test rig was developed using CAD software, as shown in Fig 1 a.

#### **3.1 Description of the test rig**

The original impact test rig consists of a sturdy base equipped with a wooden box designed to accommodate test specimens of various sizes. A vertical column features a lead screw mechanism, operated by a motor at the top, allowing for precise height adjustments as indicated by an attached scale as shown in Fig.1 b. A 500 mm long steel bar, affixed to the column, holds an adjustable electromagnet capable of securing steel balls up to 50 mm in diameter. This setup ensures that, upon release, the steel ball strikes the exact centre of the designated impact area. Additionally, protective enclosures have been added to safeguard operators from potential glass fragmentation. These enhancements enable the impact test rig to deliver more detailed and reliable assessments of glass safety, supporting the improved design and development of glass products



a) Modal of test rig      b) test rig setup      c) tested specimen of 20 mm thickness

Fig. 1 Design of Experimental setup

#### 4. TESTING METHOD AND MEASUREMENT TECHNIQUE:

The impact strength of construction materials was evaluated using a ball drop test rig designed according to ASTM F3007-13, ensuring standardized and repeatable testing. The setup includes an electromagnetic release system for precise ball drops, an adjustable lead screw mechanism for controlled drop heights, and a rigid impact surface to secure test specimens such as glass, metals, and composites. Steel balls of varying sizes 10 mm, 20 mm and 30 mm shown in Fig 1 b were used to simulate different impact forces.

The measurement system captures impact dynamics using high-speed cameras to record rebound velocity and deformation, along with microphone sensors to analyse acoustic signals. The testing procedure involves preparing specimens, selecting drop heights, and releasing the ball under gravitational acceleration. Data from cameras and sensors are analysed to determine rebound velocity, energy absorption, and failure modes such as cracks or plastic deformation. Compliance with ASTM F3007-13 ensures reliable impact resistance evaluation, supporting material selection and safety assessments in construction, automotive, and aerospace industries.

##### 4.1 The assumptions of this work are as follows:

- The impact between the ball and the material surface follows elastic or elastoplastic behavior based on material properties.
- Air resistance and other external forces are negligible during free-fall and rebound motion.

- The material properties remain consistent throughout the tests, with no significant variations in density or surface integrity.
- The test rig provides precise and repeatable drop conditions, ensuring uniform impact velocity.
- Measurement uncertainties are minimal and do not significantly affect the overall accuracy of the results.
- FEM simulations accurately represent real-world conditions, assuming ideal material behavior and boundary conditions.

**4.2 Experimental Results:**

The experiment was conducted on a 20 mm glass panel using a ball drop test with a 64-gram (30 mm size) steel ball, following ASTM F3007-13 standards. The ball was released from 1 meter height in free fall, ensuring a rectilinear impact path onto the glass specimen. Upon collision, the ball rebounded, and its rebound height and time were measured using video and audio recordings as shown in Fig. 2(a) and (b). The tested specimens was shown in fig1(c). The study analysed the impact behaviour of steel balls with diameters of 10 mm, 20 mm, and 30 mm to assess glass panel failure characteristics under varying impact forces.

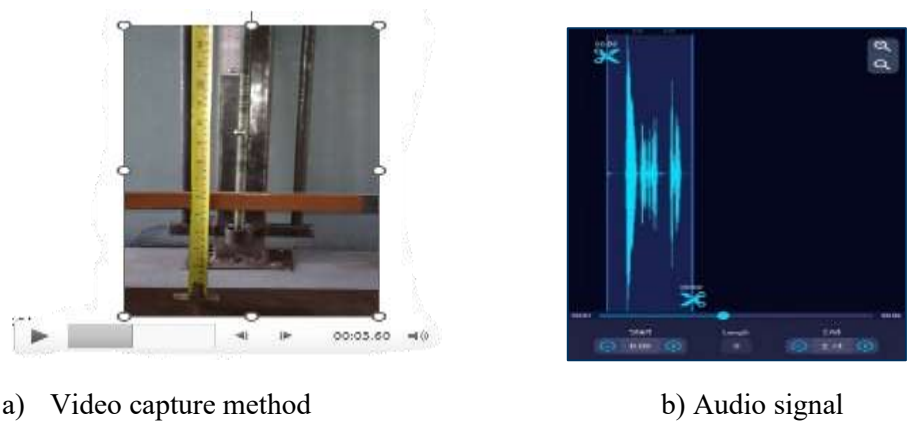


Fig. 2 Measurement Techniques

Table 1. Rebound Velocity Measurement Using Recorded Video Signal

S.NO	Size of the ball $\phi$ (mm)	Ball Weight (kg)	Impact Energy (J)	Time (s)	Rebound velocity (m/s)
1	10	0.017	0.166	0.25	2.48
2	20	0.032	0.312	0.21	2.14
3	30	0.064	0.624	0.17	1.68

Table 2. Rebound Velocity Measurement Using Recorded Audio Signal

S.NO	Size of the ball $\phi$ (mm)	Ball Weight (kg)	Impact Energy (J)	Time (s)	Rebound velocity (m/s)
1	10	0.017	0.166	0.27	2.65
2	20	0.032	0.312	0.24	2.35
3	30	0.064	0.624	0.18	1.77

### 4.3 Results and Discussion

The rebound velocity of steel balls impacting a 20 mm thick glass panel was determined using both audio signal analysis and high-speed video recordings. The objective was to compare these two digital measurement techniques and evaluate their accuracy in determining post-impact velocities. The experimental results reveal a clear size-dependent variation in rebound velocity, indicating the influence of mass, energy dissipation, and material response to impact.

#### 4.3.1 Effect of Ball Size on Rebound Velocity

From the audio signal measurements, the 10 mm ball exhibited the highest rebound velocity (2.65 m/s), followed by the 20 mm ball (2.35 m/s), and the 30 mm ball (1.77 m/s). The video-based measurements followed a similar trend, though with slightly lower rebound velocities: 2.48 m/s for the 10 mm ball, 2.14 m/s for the 20 mm ball, and 1.68 m/s for the 30 mm ball. The general decrease in rebound velocity with increasing ball size can be attributed to the relationship between mass and energy absorption.

Smaller balls, due to their lower mass, tend to store less impact energy and dissipate less energy through deformation and internal damping, leading to higher rebound velocities. Conversely, larger balls, having greater mass and impact force, induce higher stresses on the glass panel. This results in more significant energy dissipation due to internal microfractures, viscoelastic damping, and localized plastic deformation at the contact point. The reduced elasticity in the impact region leads to lower rebound velocities for larger balls.

#### 4.3.2 Comparison of Audio Signal and Video-Based Measurements

Although both measurement techniques followed the same trend, the rebound velocities determined from video recordings were consistently lower than those from the audio-based method. This discrepancy arises due to several factors:

##### 4.3.2.1 Frame Rate Limitations in Video Recording:

Cameras operate at discrete frame rates, meaning that velocity calculations are subject to interpolation errors between frames. The precision of velocity measurement depends on the frame rate; higher speeds require ultra-high-frame-rate cameras to minimize error.

##### 4.3.2.2 Audio Signal Processing Accuracy:

The audio method records impact events with a high temporal resolution, as sound waves travel much faster than visual frames update. However, it is susceptible to minor processing delays and background noise interference, which can introduce slight deviations in the calculated velocities.

#### **4.3.3 Experimental Uncertainties:**

Factors such as slight variations in ball positioning, surface roughness at the impact site, and minute deviations in drop height could contribute to measurement inconsistencies. These experimental uncertainties emphasize the need for careful calibration and alignment of both measurement techniques.

#### **4.3.4 Energy Dissipation Mechanisms**

The observed variations in rebound velocity also highlight the different energy dissipation mechanisms during impact. When a steel ball strikes the glass panel, part of its kinetic energy is transformed into:

- Elastic energy, which contributes to rebound,
- Plastic deformation and micro fracturing, which permanently alters the material's structure,
- Acoustic and thermal energy, which dissipates as sound and heat.

Larger balls, due to their greater momentum, induce higher stress concentrations, leading to more significant plastic deformation and micro fracturing at the impact site. This explains why the 30 mm ball exhibits the lowest rebound velocity, as more energy is lost through irreversible damage to the glass.

The results confirm the reliability of both digital measurement methods, with minor variations attributable to instrument precision.

### **5. DROP TEST SIMULATION USING FEM**

The drop test simulation using LS-DYNA was conducted to analyze the rebound velocity and failure behavior of the same size 20 mm thick glass panel impacted by steel balls of 10 mm, 20 mm, and 30 mm diameters. The simulation replicated experimental conditions as shown in Fig. 4 where the steel ball assigned with free fall velocity of -4.4 m/s when it was released from a 1-meter height under free fall due to gravity. The glass panel was constrained along its corners to simulate realistic support conditions as shown in Fig. 3, while the steel ball was modeled as a rigid body. Contact between the ball and the glass was defined. High-resolution meshing was applied to improve accuracy, and a brittle material model was assigned to the glass to account for fracture initiation and propagation. Simulation outputs included velocity profiles as shown in Fig. 5 and failure modes were analyzed.

The results from the simulation were compared with experimental high-speed camera and microphone sensor data, confirming that the numerical predictions closely matched physical test outcomes. The rebound velocity of the steel ball was measured at different time steps,



showing variations based on ball size and impact energy as shown in fig.6. The maximum stress regions observed in the simulation corresponded with actual fracture locations recorded in the experiments. Furthermore, the coefficient of restitution ( $e = v_1/v_0$ ) was validated, demonstrating consistency between finite element analysis (FEA) and real-world impact tests. The study highlights the effectiveness of LS-DYNA in predicting impact resistance, providing valuable insights for material design improvements in construction, automotive, and aerospace applications where impact durability is critical.

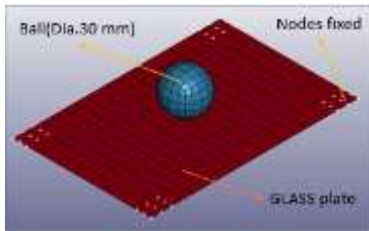


Fig. 3 FE Model of ball and Glass plate

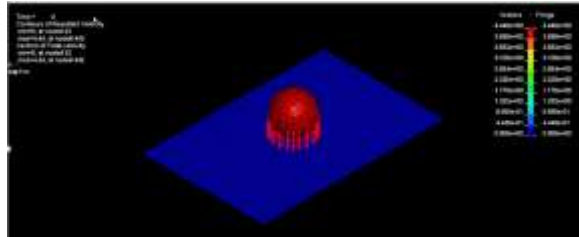


Fig. 4 Initial condition of ball drop test

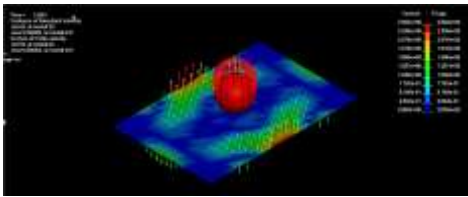


Fig. 5 Vector plot of velocity profile after rebound simulation

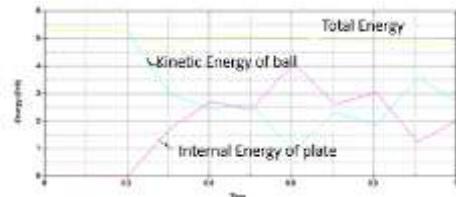


Fig. 6 Energy plot of drop test

## 6. EXPERIMENTAL VALIDATION AND NUMERICAL SIMULATION

The comparison of experimental results and finite element modeling (FEM) simulations in ANSYS LS Dyna demonstrates strong agreement in rebound velocity measurements, validating the accuracy of both approaches. The recorded video and audio signals provided real-time experimental data, while FEM simulations incorporated material properties, contact interactions, and boundary conditions to predict impact behavior as shown in Table 3, minor deviations were observed between experimental and simulated results, primarily due to material inconsistencies, measurement uncertainties, and environmental factors. However, the close correlation across all three methods confirms the reliability of FEM simulations in predicting rebound characteristics. This validation enhances the credibility of numerical modeling as a predictive tool for assessing impact resistance and structural integrity in various materials.

Table 3. Rebound Velocity Measurement Using Recorded Audio Signal

S.NO	Size of the ball (mm)	Ball Weight (kg)	Rebound velocity (m/s)		
			Video	Audio	FEM simulation



1	10	0.017	2.48	2.65	2.75
2	20	0.032	2.14	2.35	2.43
3	30	0.064	1.68	1.77	1.92

## 7. CONCLUSION

The impact strength measurement rig developed in compliance with ASTM F3007-13, provides a standardized and reliable framework for assessing the impact resistance of construction materials. By integrating high-speed cameras and microphone sensors, the rig ensures precise data acquisition for analysing impact behaviour. The strong correlation between experimental results and FEM (ANSYS) simulations confirms the rig's effectiveness in predicting rebound velocity. Minor deviations observed between experimental and numerical results are primarily due to material inconsistencies and measurement uncertainties, highlighting the importance of further refinement in calibration and testing procedures. These findings contribute to the optimization of material selection, structural safety assessments, and impact-resistant design strategies in the construction industry. Additionally, the study underscores the potential for future advancements in digital measurement techniques and impact testing methodologies, enhancing the reliability and applicability of numerical simulations in material evaluation.

## 8. APPLICATIONS AND FUTURE DEVELOPMENTS

The findings from this study contribute to enhancing safety standards and optimizing material properties in industries such as construction, automotive, and aerospace, where impact resistance is crucial. By understanding material behaviour under dynamic loading, engineers can develop more durable and resilient materials to mitigate failure risks. Additionally, the integration of AI and machine learning in impact testing can enable real-time data analysis, pattern recognition, and predictive modeling, improving the accuracy and efficiency of material assessment. Future advancements in test rig design will focus on automated data acquisition, adaptive testing mechanisms, and enhanced sensor integration, allowing for more precise and standardized impact evaluations across a broader range of materials and applications.

## Acknowledgement

The authors sincerely acknowledge the support and enthusiasm of the undergraduate students Kavi Mathi K, Akilesh M and Charunika A of the Department of Mechanical Engineering at Kumaraguru College of Technology, whose involvement in conducting the experiments and data collection greatly contributed to the successful completion of this research. Their dedication, teamwork, and keen interest in hands-on learning made this study both productive and enriching.

## 9. REFERENCE:

1. Ge, J., Li, G.-Q., & Chen, S.-W. (2012). Theoretical and experimental investigation on fragment behavior of architectural glass panel under blast loading. *Engineering Failure Analysis*, 26, 293–303. <https://doi.org/10.1016/j.engfailanal.2012.07.022>

2. Sunarno, Z. (n.d.). Impact test analysis on steel metal materials and aluminium. International Journal of Scientific Research. Retrieved from <http://ijsr.internationaljournallabs.com/index.php/ijsr>
3. Thomas, R. J., & Sorensen, A. D. (2018). Charpy impact test methods for cementitious composites: Review and commentary. *Journal of Testing and Evaluation*, 46(6), 2422–2430. <https://doi.org/10.1520/JTE20170057>
4. Patterson, A. E., Pereira, T. R., Allison, J. T., & Messimer, S. L. (2021). IZOD impact properties of full density fused deposition modeling polymer materials with respect to raster angle and print orientation. *Proceedings of the Institution of Mechanical Engineers, Part C: Journal of Mechanical Engineering Science*, 235(10), 1891–1908. <https://doi.org/10.1177/0954406219840385>
5. Jurecki, R., Pokropiński, E., Więckowski, D., & Żołądek, Ł. (2017). Design of a test rig for the examination of mechanical properties of rolling bearings. *Management Systems in Production Engineering*, 25(1), 22–28. <https://doi.org/10.1515/mspe-2017-0003>
6. Pisano, G., Bonati, A., & Royer-Carfagni, G. (2021). The effect of size and stress state on the strength of architectural glass. Experiments versus theory. *Construction and Building Materials*, 283, 122635. <https://doi.org/10.1016/j.conbuildmat.2021.122635>
7. Yazhou, B., Gang, Y., Yong, S., Hongjun, Y., & Hailin, X. (2020, July). Research on the relationship between the rigidity of cover glass and the damage of LCD in the drop test of whole machine. 2020 IEEE International Symposium on the Physical and Failure Analysis of Integrated Circuits (IPFA), 1–3. <https://doi.org/10.1109/IPFA49335.2020.9260978>
8. Kim, H.-S., Ha, B.-K., Yoo, B., Jeong, H.-S., & Park, S.-H. (2022). Numerical prediction of dynamic fracture strength of edge-mounted non-symmetric tempered glass panels under steel ball drop impact. *Journal of Materials Research and Technology*, 17, 270–281. <https://doi.org/10.1016/j.jmrt.2021.12.134>
9. Xue, L., Liu, D., Lee, H., Yu, D., Chaparala, S., & Park, S. (2013, July). An experimental and numerical study of the behavior of the thin glass edge under ball drop impact. *Proceedings of the ASME 2013 International Technical Conference and Exhibition on Packaging and Integration of Electronic and Photonic Microsystems (IPACK2013)*. <https://doi.org/10.1115/IPACK2013-73293>
10. Acar, U., Bayram, B., Cetin, H. I., & Sanli, F. B. (2012). Determining the technical standards of ping pong table by using close range photogrammetry. *The International Archives of the Photogrammetry, Remote Sensing and Spatial Information Sciences*, XXXIX-B5, 1–4. <https://doi.org/10.5194/isprsarchives-XXXIX-B5-1-2012>
11. Yang, X., Zhang, G., Yu, Y., Yu, Q., Lei, M., & Ding, B. (2021). Factors influencing the coefficient of restitution in rockfall impacts. *Natural Hazards Review*, 22(3). [https://doi.org/10.1061/\(ASCE\)NH.1527-6996.0000454](https://doi.org/10.1061/(ASCE)NH.1527-6996.0000454)
12. Basson, F., Humphreys, R., & Temmu, A. (2013). Coefficient of restitution for rigid body dynamics modelling from onsite experimental data. *Proceedings of the 2013 International Symposium on Slope Stability in Open Pit Mining and Civil Engineering*, 1161–1170. [https://doi.org/10.36487/ACG\\_rep/1308\\_82\\_Basson](https://doi.org/10.36487/ACG_rep/1308_82_Basson)
13. Harnsoongnoen, S., Srisai, S., Kongkeaw, P., & Rakdee, T. (2024). Improved accuracy in determining the acceleration due to gravity in free fall experiments using smartphones and mechanical switches. *Applied Sciences*, 14(6), 2632. <https://doi.org/10.3390/app14062632>
14. Qiao, P., Yang, M., & Bobaru, F. (2008). Impact mechanics and high-energy absorbing materials: Review. *Journal of Aerospace Engineering*, 21(4), 235–248. [https://doi.org/10.1061/\(ASCE\)0893-1321\(2008\)21:4\(235\)](https://doi.org/10.1061/(ASCE)0893-1321(2008)21:4(235))
15. Zafar, U., Hare, C., Hassanpour, A., & Ghadiri, M. (2014). Drop test: A new method to measure the particle adhesion force. *Powder Technology*, 264, 236–241. <https://doi.org/10.1016/j.powtec.2014.04.022>
16. S. Senthil Murugan (2020), Mechanical properties of materials: Definition, testing and application. *International Journal of Modern Studies in Mechanical Engineering (IJMSME)* Volume 6, Issue 2, PP 28–38, <http://doi.org/10.20431/2454-9711.0602003>
17. Sandeep, C. S., Luo, L., & Senetakis, K. (2020). Effect of grain size and surface roughness on the normal coefficient of restitution of single grains. *Materials*, 13(4), 814. <https://doi.org/10.3390/ma13040814>
18. Yang, J., Silvestro, C., Khatri, D., De Nardo, L., & Daraio, C. (2011). Interaction of highly nonlinear solitary waves with linear elastic media. *Physical Review E*, 83(4), 046606. <https://doi.org/10.1103/PhysRevE.83.046606>
19. C.S. Sandeep, K. Senetakis, D. Cheung, C.E. Choi, Y. Wang, M.R. Coop, C.W.W. Ng(2020), Experimental study on the coefficient of restitution of grain against block interfaces for natural and engineered materials, *Canadian Geotechnical Journal*, Volume 58, Issue 1, Pages 35–48, <https://doi.org/10.1139/cgj-2018-0712>.